



Efficient parameter identification in nonlinear multi-body dynamics through frequency response and harmonic distortion analysis

Kevin Steinbach^{1,2,3} · Dominik Lechler¹ · Peter Kraemer² · Iris Gross³ · Dirk Reith^{3,4}

Received: 16 May 2025 / Accepted: 29 July 2025
© The Author(s) 2025

Abstract

This paper presents a methodology to identify sensitive parameters in nonlinear multi-body dynamic systems. It aims to reduce computational cost by minimising the number of numeric calculations required for statistical evaluation, while reliably identifying significant influencing parameters. The proposed approach consists of three major steps: In the first step, a design space analysis based on the frequency response function pre-filters parameters with negligible influence. It verifies the model's validity across the parameter space for linear dependencies. The second step applies the design of experiments based on the total harmonic distortion to investigate the nonlinear effects of the retained parameters. The third step uses a multiple linear regression analysis to estimate and validate the non-measurable or virtual parameters by identifying linear and multifactorial relationships. This integrated approach reduces the required number of simulations, while the application of the frequency response function and the total harmonic distortion as part of a cost function enables robust statistical evaluations. The methodology is validated by comparing simulation and experiment using a consistent setup, in which a small shaker excites the system with a logarithmic chirp signal. The resulting spectrograms of simulated and measured acceleration signals reveal comparable trends, including observable higher harmonics. These similarities indicate the validity of the method, while discrepancies in the absolute values between simulation and experiment can be attributed to inaccurate model assumptions. Thus, future research could consider testing a simplified or refined benchmark system to further investigate the applicability of the approach.

Keywords Multi-body dynamics · Parameter identification · Sensitivity analysis · Design of experiments · Frequency response function · Harmonic distortion

✉ K. Steinbach
steinbach.research@gmx.net

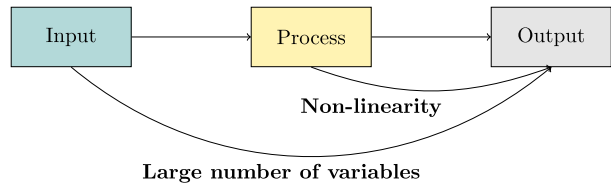
¹ Engineering Platform Drive Unit, Robert Bosch GmbH, eBike Systems, Reutlingen, 72770, Germany

² Department of Mechanical Engineering, University of Siegen, Siegen, 57076, Germany

³ Institute of Technology, Resource and Energy-efficient Engineering (TREE), University of Applied Science Bonn-Rhein-Sieg, Sankt Augustin, 53757, Germany

⁴ Fraunhofer Institute for Algorithms and Scientific Computing (SCAI), Sankt Augustin, 53757, Germany

Fig. 1 Schematic system description of a system with a multitude of parameters and a non-linear behaviour



1 Introduction

In the context of modelling and simulation of systems, a significant challenge lies in accurately determining the appropriate parameter values after selecting the modelling techniques and establishing the boundaries. A crucial aspect of this process is the efficient acquisition and validation of these parameter values. While numerous methods may exist for estimating individual parameters, complications arise as the complexity of the parameter set increases. The time required to pursue each parameter can be prohibitive, even when specific solution approaches are available, as these often require extensive knowledge and expertise or involve substantial costs and specialised equipment. Additionally, specific parameter values, such as virtual parameters, may not be physically measurable. Instead, they serve as approximations of physical behaviour and need to be estimated.

When it comes to (*elastic*) multi-body dynamic (eMBD) systems that involve contacts, most probably a nonlinear behaviour emerges. This results in a problem due to both the large number of parameters, which themselves need to be validated and the nonlinear system behaviour as well. Through the nonlinearity of the process, the ratio of input and output is non-proportional, and an interaction of parameter combinations may lead to divergent results in contrast to a single parameter change. Figure 1 illustrates this dependency.

Single parameters can be determined and used for validation with measured data. For instance, one can weigh the mass of a single component, obtain the natural modes and frequencies using experimental modal analysis, and gain the stiffness caused by elastic material properties through a quasi-static load test. Even though it is possible to obtain parameter sizes like these and to incorporate the nonlinear nature of the system, there are further parameters that cannot be measured directly and, hence, can only be estimated. Since they may additionally influence the process, the question arises, how to prove the correctness of the model assumptions, including these parameters? To address this question, various techniques can be employed, which can be categorised as follows, to the best of our knowledge. The sources given serve as examples for each case and do not claim to be exhaustive.

- *Comparison of analytical or experimental results*: This technique considers a quantitative comparison between discrete values. For example, Pigorini et al. [1] compare the multi-body dynamic model against experimentally measured velocity data, displacements, and forces over time, while Parra et al. [2] include additional vehicle quantities, such as angles and accelerations, during tested driving manoeuvres. This allows an efficient validation, assuming similar boundary conditions.
- *Analysis of assumptions and parameters*: A more generalised approach is to prove the assumptions and choices of parameters used for the modelling process. For instance, Klogprogge et al. [3] perform an assessment based on a pedigree matrix to systematically identify and evaluate the key assumptions within the modelling framework, with a particular focus on their potential lack of validity. Using a flexible approach instead of rigid bodies would also be a suitable example. In contrast, various numbers of parameter values are typically examined in terms of sensitivity and robustness.

- *Sensitivity analysis and robustness interpretation*: The sensitivity analysis allows for identifying the most important parameters, while the robustness interpretation further analyses whether the model can be trusted, in terms of stable statements, even under realistic uncertainties. For instance, Smith et al. [4] present various sensitivity techniques, emphasising their use for model validation, while Dimov et al. [5] apply the Monte Carlo method to investigate the model behaviour under statistical deviations.
- *Frequency and stability analysis*: The frequency and stability analysis are used to identify the dynamic system behaviour. While the frequency analysis evaluates critical frequencies, the stability analysis aims to identify the inherent dynamics of the system model. For instance, Gatti et al. [6] investigate the frequency response and stability via the harmonic balance method, and Carri et al. [7] use the frequency response function and reserve path method to analyse nonlinear structures. Luo et al. [8] utilise bifurcation and stability analysis in nonlinear dynamical systems for characterisation.
- *Numerical consistency and convergence studies*: In numerical analysis, discretisation transforms a differential equation into a computable form [9]. Therefore, consistency indicates how accurately the discrete problem reflects the original one, and convergence indicates how stable the solution remains under small perturbations [9]. The aim is to implement and apply a suitable numerical solver method and select a suitable error tolerance. For instance, Bauchau et al. [10] apply time integration schemes that incorporate both energy-preserving and energy-dissipating approaches, along with automated time step selection, to solve the dynamic simulation of flexible, nonlinear multi-body systems.
- *Hybrid or data-driven validation approaches*: As hybrid we categorise approaches that either include more than one of the mentioned methods or supplement them with unique means and procedures. Especially, the data-driven validation may include experimental data but categorise a broader field, such as statistical methods, machine learning algorithms, or other data-driven procedures. For instance, Renardy et al. [11] scale a 2D output to a 3D enabling a comparison to real measurement data, Mokhtari and Imanpour [12] use a data-driven model based on experimental and numerical data, which could be used for validation, and Zhang et al. [13] perform a statistical analysis over 600 measurements to validate the multi-body contact modelling of a hub-bearing.

It must be emphasised that no one-size-fits-all solution exists that can be universally applied. The challenge in this context lies in the large number of influencing parameters combined with the nonlinear behaviour of the system (see Fig. 1), which predominantly arises from contacts. Therefore, a method is proposed that can be applied to nonlinear systems, combining sensitivity analysis with frequency analysis based on numerical data. Using the proposed method, the problem size can be reduced while nonlinear dependencies can be included for the sensitivity analysis. The novelty of this approach is the combination of existing methods as follows: the frequency response function is used within a design space analysis to narrow down the initial problem size, while additionally the total harmonic distortion is used in a full factorial design of experiments to capture the nonlinear dependencies on both, the signal itself and within the parameter interactions themselves. The robustness is proved by multiple linear regression. Additionally, the proposed method is validated using experimental data.

Compared to nonlinear identification method as categorised by Kerschen et al. [14] (linearisation techniques, time-domain methods, frequency-domain methods, modal methods, time–frequency analysis, black-box modelling, and structural model updating) the method can be positioned as a hybrid approach. It incorporates elements of linearisation and frequency-domain techniques, with a primary focus on parameter identification and sensitivity analysis. This is in contrast to system characterisation techniques through decomposition

methods, such as the Hilbert transform, since the evaluation of the signal behaviour itself is not the focus.

The proposed methodology is primarily suitable for analysing systems in which nonlinearities predominantly arise from contact interactions. The underlying assumptions rely on linearised frequency response functions and harmonic distortion metrics, which assume small movements and perturbations around an equilibrium or a nominal operating point. For motions with large amplitude, these assumptions lose validity due to highly nonlinear behaviour, such that the frequency response function (FRF) becomes inadequate and the total harmonic distortion (THD) may no longer represent meaningful parameter sensitivities.

2 Methodology

2.1 Brief theory of contacts in multi-body dynamics

The mechanical system is modelled as a multi-body system, optionally incorporating modal reduced bodies to account for structural flexibility. The resulting equations of motion are represented as a differential ordinary equation of the second order, or algebraic, respectively, in case of constraining conditions:

$$\mathbf{M}\ddot{\mathbf{q}} + \mathbf{D}\dot{\mathbf{q}} + \mathbf{K}\mathbf{q} = \mathbf{F}_{\text{ext}}(t) + \mathbf{F}_{\text{contact}}(\mathbf{q}, \dot{\mathbf{q}}) \quad (1)$$

Here, \mathbf{q} denotes the generalised coordinates, which include rigid body motions and selected elastic modes. The matrices \mathbf{M} , \mathbf{D} , and \mathbf{K} represent the mass, damping, and stiffness matrices, respectively. The vector \mathbf{F}_{ext} contains external forces, such as a shaker excitation (as used later), and $\mathbf{F}_{\text{contact}}$ the total contact forces. According to Hunt and Crossley [15], the contact normal force can be described as a viscoelastic term, where the restitution is described as viscous damping. Thereby, the contact normal force F_N introduces an inequality, in which the resulting force depends on the penetration in normal direction $\delta(\mathbf{q})$ on its time derivative as follows:

$$\mathbf{F}_{N,i} = \begin{cases} 0, & \text{if } \delta < 0 \\ k \delta^b + c \dot{\delta} \mu(\delta), & \text{if } \delta \geq 0 \end{cases} \quad (2)$$

with assumed Coulomb friction as

$$F_{T,i} = -\frac{v_G}{|v_G|} \mu_S F_{N,i} \quad (3)$$

This formula represents one common interpretation of contact modelling with dry friction in multi-body dynamic systems [16], whereby alternative formulations exist, such as *Kelvin-Voigt* or the more complex *LuGre*, to mention a few (compare [17–19]). It should be noted that these models do not capture elasto-hydrodynamic contact and thus represent a simplified approximation, which is considered acceptable due to the low relative speed in the applied model. Moreover, the specific choice of contact model is of minor importance for the scope of this work.

The total contact force consists of Equation (2) and (3) over the sum of contacts n

$$\mathbf{F}_{\text{contact}} = \sum_{i=1}^n \mathbf{H}_i^T (\mathbf{F}_{N,i} + \mathbf{F}_{T,i}) \quad (4)$$

Fig. 2 Illustration of the contact areas of the output shaft

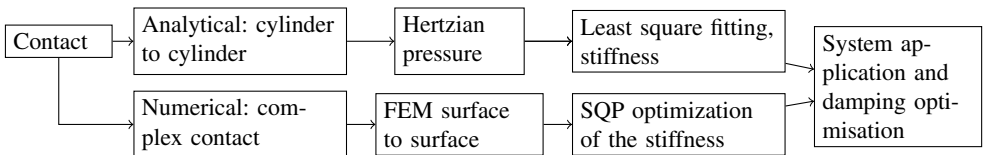
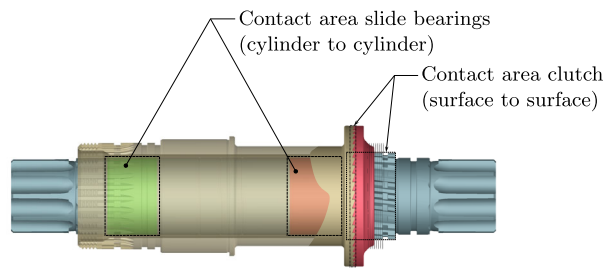


Fig. 3 Methodology for contact modelling to determine stiffness and damping parameters

where \mathbf{H}_i^T symbolises a transformation matrix which projects the force at a contact point i onto the global degrees of freedom of the multi-body system. A more detailed description can be obtained from [16]. All in all, the normal contact force, in addition to the frictional force, induces a non-linear behaviour caused by the contact stiffness. Additionally, this is also valid for the damping coefficient, in the case that it is variable.

2.2 Model development

The nested configuration of the shaft assembly, as applied in the system, highlights the critical role of contact areas in the overall system behaviour (see Fig. 2). While relative movements during operation under load are assumed to be minimal, the contact stiffness resulting from material pairing, geometry, and clearance can still facilitate vibrations across multiple bodies.

In this model, contact areas — whether specific regions or entire bodies — are treated as rigid. Elastic effects are captured through the induced contact stiffness, while contact locations are determined using a non-deformable geometric representation. It is assumed that the relative motion between the sliding bearings is negligible, as the clutch either locks relative rotation or operates at a maximum frequency of 2 Hz in this particular case. The bearings are self-lubricating, leading to the assumption of dry friction. Thus, a quasi-static contact model is adopted, neglecting the effects of elastohydrodynamic lubrication. Similarly, dry friction is assumed for the clutch contacts due to minimal anticipated movements and light lubrication. Roller bearings are included as surrogate models to match the later experimental setup, yet are not depicted within this Figure. They also indicate a non-linear stiffness and damping, but are not further elaborated upon in this work, as they are implemented with *MSC Adams Bearing AT*.

Figure 3 illustrates the contact modelling process, in which simple cylinder-to-cylinder contacts can either be used or a numerical approximation using the finite element method (FEM).

For cylinder-to-cylinder contact, the Hertzian pressure [20] is calculated, e.g. using modifications proposed by Kunert [21], which yields a contact force [22]. This force is then approximated through regression via the least squares method. Alternatively, and for more

complex contacts, a FEM simulation can be performed as a preprocessing step, yielding the contact stiffness [23]. While experimental trials are also possible [23], they are not included in this contribution due to limited resources for a thorough investigation. Thus, although acknowledged, they do not significantly impact the findings or conclusions of this work.

The local deformation u_c is derived from the penetration in the normal direction, influenced by the resulting contact parameters, specifically the stiffness. Based on the kinematics relevant to the geometry of the bodies in contact, the global deformation u may occur in a different direction ($u \neq u_c$). This is indicated by the scaling function $g(u_c)$ in Equation (5). To overcome this problem, the identical load case, such as the one used in the FEM, needs to be applied in the multi-body dynamics (MBD) simulation. One restriction is that one contact is treated at a time. The stiffness factor k and the exponent b are fitted using a sequential quadratic programming (SQP) as an optimisation. Therefore, the reference curve of the load $F_{c,i}$, e.g. from the FEM calculation, is used and the difference to the resulting contact force $f(u_i, k, b)$ minimised while the motion u is enforced by a constraint.

$$\min_{k,b} \sum_{i=1}^n [F_{c,i} - g(u_{c,i}) \cdot k \cdot u_i^b]^2 \quad (5)$$

The SQP algorithm provides the values of k and b , which can be used for contact modelling within the MBD. This functionality may be an integral part of software, such as *MSCADS-SQP* in *MSC Adams* [24], or available through *fmincon* in *Matlab* [25]. Here, $F_{N,n}$ represents the maximum expected normal force, and the range of F_N should encompass the anticipated force interval to ensure robust fitting without extrapolation.

Once the stiffness is defined, the relevant damping needs to be determined. For the given contact, the critical damping c_{critical} is used to determine the maximum damping ratio, which builds the upper limit of the design space by

$$c_{\text{critical}} = \sqrt{\frac{k_{\text{red}}}{m_{\text{red}}}} \quad (6)$$

with the reduced contact stiffness and reduced mass, k_{red} and m_{red} , respectively.

2.3 Proposed validation approach

To overcome the limiting nature of the pure amount of input variables combined with a long calculation duration, the method presented reduces the complexity in the first instance. As a second instance, the sensitive parameters are checked in terms of their influence on the non-linear system behaviour. Finally, a regression model is used to determine a trend, allowing us to assess the robustness of the sensitive parameters. Figure 4 reveals these steps.

In principle, the procedure for the first and second instances is similar. While, through the use of design space analysis in the first instance, only linear relations are obtained by varying one parameter value at a time, the second instance, using the design of experiments, involves the interactions of the varying variables, enabling the detection of non-linear influences of parameter change. The novelty of this method lies in integrating the frequency response function on the one hand, and the total harmonic distortion on the other. These are used as quality features to build the input for the cost function of the regression model for the third instance. The precise correlation is shown in Fig. 5.

The parameter space is established through the modelling process. To define the design space, relevant parameters are hypothesised along with their limiting values, which serve

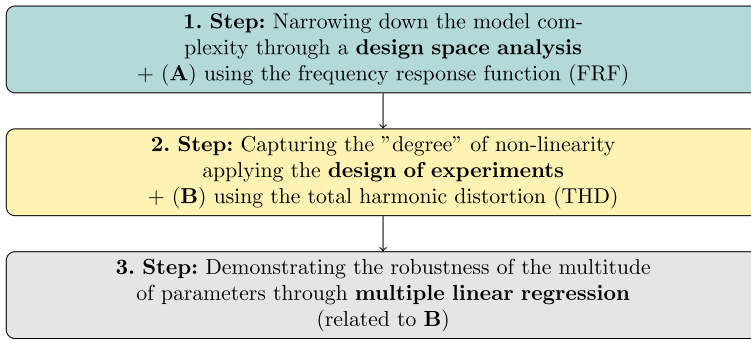


Fig. 4 Proposed method for model validation to overcome the limiting nature due to model complexity

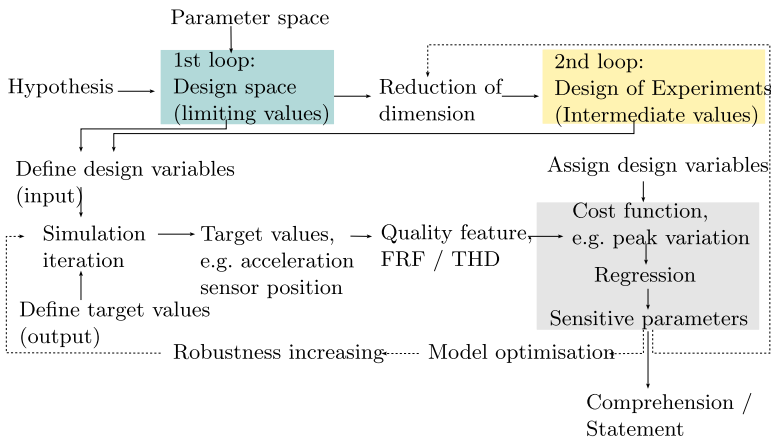


Fig. 5 More detailed description of the methodology to perform the sensitivity analysis

as inputs for the sensitivity analysis. Target values are then defined as outputs to assess the influence of these inputs. Simulation iterations are conducted for various input sizes, and the corresponding output sizes are evaluated.

To facilitate comparison of the results, a quality metric is identified, which in this paper is either the FRF or THD. However, other metrics, such as the root mean square (RMS) of acceleration, could also be utilised. This quality metric undergoes specific post-processing to yield a cost function represented as a single scalar value. Each design variable and its associated values are linked to the corresponding cost function, enabling the identification of sensitive parameters through regression analysis. To access the non-linear nature of the system, a logarithmic sinus sweep chirp signal is used as an input signal to excite the system. It has the following form and remains equal for all analyses

$$y_{\text{Chirp}}(t) = A_0 \cos \left(2\pi f_0 t \left(\frac{f_1}{f_0} \right)^{\frac{t}{T}} \right), \tag{7}$$

with the amplitude is A_0 and the logarithmic frequency increase from f_0 to f_1 within the duration T . By this, all frequencies within the given range are excited as effectively as possible,

since lower frequencies require a longer excitation time due to their longer wavelength and higher frequencies a shorter one. The yielding excitation force is then used as input signal and any sensor signal as output signals, to build the FRF using the H_v estimator according to [26] as follows

$$H_v = \frac{(\epsilon S_{xx} - S_{pp}) + \sqrt{(\epsilon S_{xx} - S_{pp})^2 + 4\epsilon S_{px} \cdot S_{xp}}}{2\epsilon S_{xp}} \quad (8)$$

with the cross power spectrum S_{px} , S_{xp} and the power spectrum of the input signal S_{pp} and output signal S_{xx}

$$S_{px} = Y \cdot \text{conj}(X); \quad S_{xp} = X \cdot \text{conj}(Y); \quad S_{pp} = |X|^2; \quad S_{xx} = |Y|^2 \quad (9)$$

and X, Y the complex Fourier transformed

$$X = \mathcal{F}\{x_{\text{out}}(t)\}; \quad Y = \mathcal{F}\{y_{\text{in}}(t)\}. \quad (10)$$

The transfer function $H_{v,i}$ for any variation (i) is then used and multiplied by $H_{v,0}$ to obtain a single scalar value as an indicator of the correlation between the two functions.

$$y_{\text{cost},i} = H_{v,i} \cdot H_{v,0}^T \quad (\text{dimension} := [1 \times N] \cdot [N \times 1]) \quad (11)$$

$H_{v,0}$ is the reference function with nominal values, or such, which shall build the base for comparison. All of that is valid for *single-input single-output* (SISO) systems.

To determine the degree of non-linearity, an approach based on total harmonic distortion is employed. Based on the principle of a single frequency (f) excitation of a non-linear system, sub-harmonic ($2f, 3f, \dots$) and super-harmonic ($\frac{1}{2}f, \frac{1}{3}f, \dots$) responses occur, depending on the underlying nonlinear behaviour [27]. In contrast, an identical excitation in a linear system evokes a harmonic response of the same frequency, typically with increased amplitude and phase shifts at resonance [28]. In theory, this means the occurrence of harmonic responses indicates a nonlinear system, and the absence of a linear system. In [29], for instance, a model that is originally linear becomes nonlinear due to the inclusion of friction effects, resulting in subharmonic responses under harmonic excitation.

To distinguish between a genuine vibration mode and harmonic distortion, it is necessary to analyse the system over a broader frequency range: When a harmonic excitation is applied at or near a natural frequency, a linear system typically responds with an increased amplitude at that frequency [30]. The frequency response then shows a smooth, bell-shaped amplitude peak, without subharmonic or superharmonic components. In contrast, nonlinear systems can exhibit amplitude-dependent resonance frequencies, which manifest as asymmetric peaks in the frequency response [31]. Moreover, nonlinearities can introduce additional frequency components, such as subharmonics or superharmonics of the excitation frequency [27]. These harmonic distortion components only appear under forced excitation and increase in magnitude with the excitation amplitude due to nonlinear effects.

To sum it up, the presence of frequency components at integer multiples of the excitation frequency may indicate either harmonic distortion or resonant modes. If these components shift when the excitation frequency is varied, they are likely due to harmonic distortion arising from system nonlinearities. If they remain fixed, they typically correspond to resonant modes and reflect linear dynamic characteristics.

In principle, the total harmonic distortion captures the resulting higher harmonic vibrations (sub-harmonics) and calculates the deviation from the base frequency as follows

$$THD = 100 \cdot \frac{\sqrt{\sum_i^n P_i^2}}{|P_1|} [\%], \quad i \geq 2 \quad (12)$$

where P_1 is the power of the base frequency and P_i is the power of each harmonic [32]. To receive the power from the time-variable logarithmic chirp signal, an *order map computation* is performed as the first step, and an *order spectrum computation* as the second step. This procedure can be found in [33] and is a standardised routine in *MATLAB Vibration Analysis*.¹ In the short term, the following operations are used according to [33]:

1. The short-time Fourier transform (STFT) is computed to obtain a time-frequency representation of the signal $x_{\text{out}}(t)$:

$$X(t, f) = \int x_{\text{out}}(\tau) e^{-j2\pi f\tau} d\tau \quad (13)$$

2. To express this representation in terms of orders n_{order} rather than frequency, the frequency axis is transformed using the rotational frequency f_r :

$$n_{\text{order}} = \frac{f}{f_r} = \frac{f}{\frac{\text{rpm}(t)}{60}} \quad (14)$$

3. Thus, the order-domain representation is:

$$X(t, n) = X\left(t, n_{\text{order}} \cdot \frac{\text{rpm}(t)}{60}\right) \quad (15)$$

which results in the order map, where the signal is represented as a function of order n and time t .

4. To compute the order spectrum, the order map is integrated over time to obtain the average power or amplitude for each order:

$$P(n) = \int |X(t, n \cdot f_r)| dt, \quad (16)$$

where $P(n)$ is the power/amplitude of order n , $X(t, n \cdot f_r)$ is the order-domain representation. This is also valid for y_{in} and Y analogous to Equation (10).

The mentioned procedure yields the order spectrum, which displays the contribution of each order n to the overall signal energy. To access this behaviour properly, the $\text{rpm}(t)$ function is obtained from the input chirp signal and has the following form

$$\text{rpm}(t) = 60 \cdot (f_0 \cdot \exp(k \cdot t)) \quad (17)$$

where k is the growth rate of the frequency increase. To apply Equation (12), the *de-trend* values of P are used, enabling a comparison, since only the relative deviation between the signals is of interest.

¹*rpmordermap(...)* and *orderspectrum(...)*.

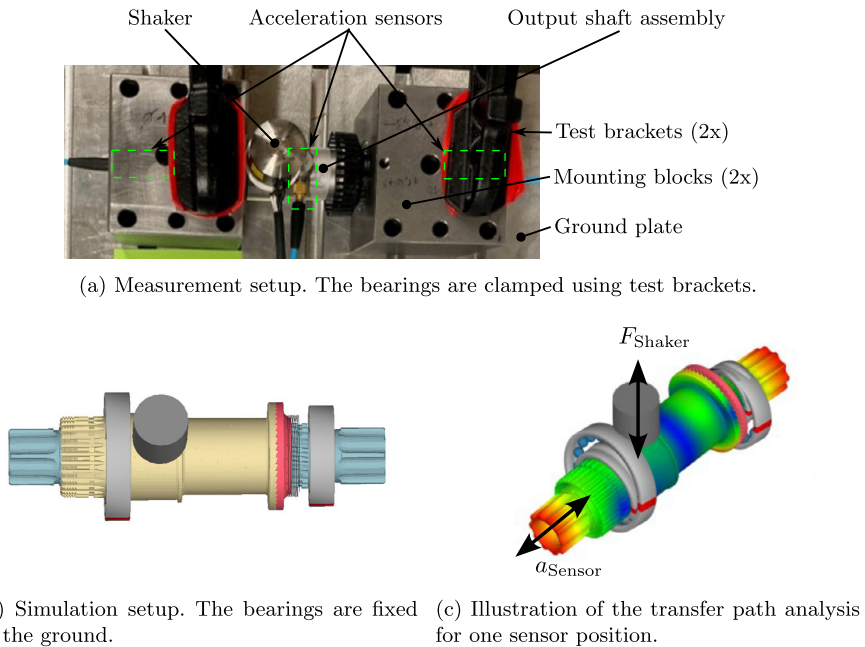


Fig. 6 Test setup with shaker and accelerometers for validating the output shaft assembly

The insights gained from this analysis can be employed to optimise highly sensitive parameters, thereby enhancing the robustness of the model. Furthermore, only decisively sensitive parameters are selected for a design of experiments (DoE), significantly reducing the dimensionality of the factors involved and minimising iteration costs. In the DoE, intermediate values are also considered, and the relationships between simultaneously altered variables are examined. However, it is constrained by the calculation efficiency, which requires the design space analysis as the first step in reduction. A model simplification could also be considered instead, but this paper assumes the case that it would not be feasible.

The final regression model applied is based on the following function, which yields the best results in our specific case.

$$y = \alpha + \sum_{i=1}^n \beta_i x_i + \sum_{i=1}^n \sum_{j=i+1}^n \beta_{n+j} \frac{x_i}{x_j} + \sum_{i=1}^n \beta_{2n+i} x_i^2 + \epsilon. \quad (18)$$

where α is the intercept, $\beta_1 \dots \beta_n$ represent the coefficients, $x_1 \dots x_n$ the design variables as input values, ϵ the error size and y the estimated solution which represents the cost function, e.g. the THD. The total amount of design variables is n .

2.4 Arrangement of experiment and simulation

To closely mimic the operational behaviour of the installed state, a test setup is designed where the system is fixed over the bearings, allowing the assembly to oscillate. A small shaker excites the system, and the acceleration of the shafts is measured at various sensor positions (see Fig. 6). The illustrated shaft assembly is part of an e-bike drive unit from previous work in [34].

For validation purposes, the shaker's mass and centre of gravity, as well as the sensor positions, are included in the model. Given the contacts between the slide bearings and the clutch, non-linearities are anticipated, prompting a transient analysis using a logarithmic chirp as described in Sect. 2.3. The testing is conducted in the time domain to account for potential non-linear effects. The known excitation signal from the logarithmic chirp serves as input (see Equation (7)), while the various spatial acceleration signals are treated as outputs.

The nested assembly of the shafts is expected to primarily exhibit rigid body modes within the frequency range up to 5 kHz. However, the influence of the bodies' elasticity must also be analysed, as structural modes may superimpose on the rigid body modes, or the yielding flexibility could affect the system behaviour, leading to mode shapes not captured by a purely rigid body approach. Due to limited access for monitoring the structure, it is not feasible to obtain a complete measurement of spatial mode deflections. Nevertheless, since rigid body modes are expected to dominate, one sensor per structure is deemed sufficient. Additionally, a FEM-based modal analysis is conducted to examine the mode shapes of both individual components and the assembly as a whole. This analysis reveals no distinct mode shapes at frequencies below 5 kHz.

3 Results

3.1 Design space analysis

In total, there are 19 parameters defined as design variables, whose minimum and maximum values span the design space. The resulting limits are defined either through physically given restrictions or through such a broad dispersion of virtual parameter sizes that, conversely, a sensitivity can be excluded, presuming a negligible change in the results. Table 1 lists the relevant parameters, their limiting values, and describes the origin of the assumptions behind the values.

According to the methodology presented in Sect. 2.3, the design space is analysed by changing one design variable at a time while keeping the others' nominal values. The only exceptions are the slide bearings' *static and dynamic friction coefficient*, the *stiction and friction velocity*, and the *bearing's preload*, which are changed as a pair each to comply with the underlying mathematical model. Their influence becomes visible when reviewing the FRFs.

Figure 7 presents the FRFs from the radial shaker force to the axial crank shaft acceleration out of the simulated results for each modified parameter value. To include further parameters or analyse different target values is also possible by this method and may lead to divergent results. Yet, a pre-study of the FRFs revealed that the consideration of the inner shaft acceleration in axial direction is the most dominant one and hence used without further notice.

It is visible that the FRF aligns with the reference significantly for some parameter values, whereas others either shift the resonance peaks or increase the total power level. To evaluate the results, the scalar product of the magnitude of both curves, the reference one and each one with modified parameters, is used. The magnitude values of the curves are considered in decibel units for the calculation, which enables the incorporation of both small and large changes. The resulting scalar factor indicates the concurrence. All factors combined and normalised form the sensitivity matrix, which is shown as a bar plot in Fig. 8.

The bar plot reveals that all but six parameters have an influence of less than 10% on the results. For the sake of clarity, only some of the contributing parameter sizes are exemplarily

Table 1 Reference values of the design space analysis

| Parameter | Minimum | Nominal | Maximum | Comment |
|----------------------------|---|---|---|-------------------------|
| Slide bearing | | | | |
| Static coefficient | 0.05 | 0.10 | 0.15 | Literature values |
| Dynamic coefficient | 0.02 | 0.05 | 0.10 | Literature values |
| Stiction velocity | 0.1 mm s ⁻¹ | 1.0 mm s ⁻¹ | 10.0 mm s ⁻¹ | Factor 10 |
| Friction velocity | 0.01 mm s ⁻¹ | 0.1 mm s ⁻¹ | 1.0 mm s ⁻¹ | Factor 10 |
| Stiffness coefficient | 7.05 × 10 ⁴ N mm ⁻¹ | 7.05 × 10 ⁵ N mm ⁻¹ | 7.05 × 10 ⁶ N mm ⁻¹ | Factor 10 |
| Stiffness exponent | 1.20 | 1.33 | 1.46 | ±10% |
| Radial clearance | 1 × 10 ⁻³ mm | 5 × 10 ⁻³ mm | 1 × 10 ⁻² mm | estimated |
| Damping coefficient | 1 N mms ⁻¹ | 234 N mm s ⁻¹ | 468 N mm s ⁻¹ | Derived from c_{crit} |
| Clutch - Spring | | | | |
| Stiffness coefficient | 0.15 N mm ⁻¹ | 0.3 N mm ⁻¹ | 0.45 N mm ⁻¹ | Construction values |
| Damping coefficient | 1 × 10 ⁻⁴ N mms ⁻¹ | 1 × 10 ⁻³ N mm s ⁻¹ | 1 × 10 ⁻² N mm s ⁻¹ | Factor 10 |
| Clutch - Driveshaft | | | | |
| Stiffness coefficient | 3.14 × 10 ⁵ N mm ⁻¹ | 3.14 × 10 ⁶ N mm ⁻¹ | 3.14 × 10 ⁷ N mm ⁻¹ | Factor 10 |
| Stiffness exponent | 1.18 | 1.31 | 1.44 | ±10% |
| Damping coefficient | 1 N mm s ⁻¹ | 257.3 N mm s ⁻¹ | 514.6 N mm s ⁻¹ | Derived from c_{crit} |
| Clutch - Crankshaft | | | | |
| Stiffness coefficient | 7.78 × 10 ³ N mm ⁻¹ | 7.78 × 10 ⁴ N mm ⁻¹ | 7.78 × 10 ⁵ N mm ⁻¹ | Factor 10 |
| Stiffness exponent | 0.89 | 0.99 | 1.09 | ±10% |
| Damping coefficient | 1.0 N mm s ⁻¹ | 40.5 N mm s ⁻¹ | 81.0 N mm s ⁻¹ | Derived from c_{crit} |
| Bearing L1 | | | | |
| Radial clearance | 1 × 10 ⁻³ mm | 5 × 10 ⁻³ mm | 1 × 10 ⁻² mm | Construction values |
| Damping coefficient | 1 × 10 ⁻³ N mms ⁻¹ | 1 × 10 ⁻² N mm s ⁻¹ | 1 × 10 ⁻¹ N mm s ⁻¹ | Factor 10 |
| Bearing L3 | | | | |
| Radial clearance | 1 × 10 ⁻³ mm | 5 × 10 ⁻³ mm | 1 × 10 ⁻² mm | Construction values |
| Damping coefficient | 1 × 10 ⁻³ N mms ⁻¹ | 1 × 10 ⁻² N mm s ⁻¹ | 1 × 10 ⁻¹ N mm s ⁻¹ | Factor 10 |

presented in Fig. 7. An increase or decrease of a value may have a different effect, e.g. the slide bearing damping of 1 N mm s⁻¹ leads to a change in results of ≈35%, whereas a value of 468 N mm s⁻¹ leads to less than 1%.

The six most dominant parameters are: the (axial) preload of the bearings, the clutch contact stiffness to the drive shaft and also its damping, the damping of the slide bearings, the slide bearing stiction and friction velocity, and the slide bearing dynamic stiction and friction coefficient. The amount of design variables is further reduced, since one calculation duration is around 90 min and the problem size of a full factorial design of experiments increases exponentially with $\mathcal{O}(d^n)$, where d is the number of parameter values and n the amount of design variables. Therefore, the design space is reduced by delimiting the preload as a separate analysis, as Sect. 3.3 reveals its influence. Additionally, the stiction and friction coefficients are considered, as their influence is lower compared to the other factors. Otherwise, instead of full-factorial DoE, other types of implementations could be used, which have not been further tested.

Fig. 7 Exemplary presentation of the FRFs from shaker to crankshaft acceleration with 1% to 5% deviation from the reference curve

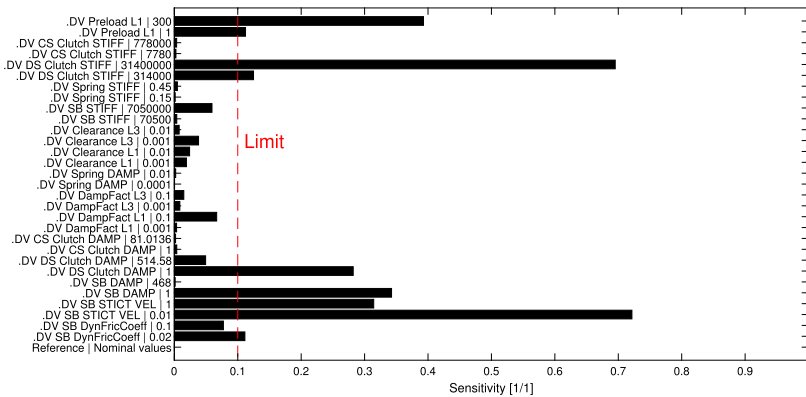
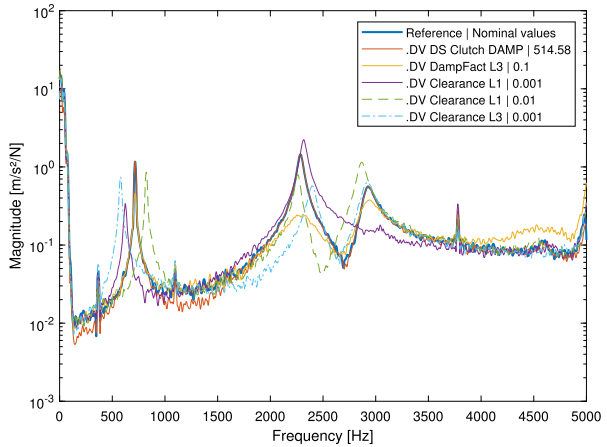


Fig. 8 Resulting sensitivity built out of the scalar from the current FRF to the reference with subsequent normalisation

Table 2 Table listing the factors of the DoE analysis. Three values per design variable yield $3^4 = 81$ simulations, using a full-factorial setup

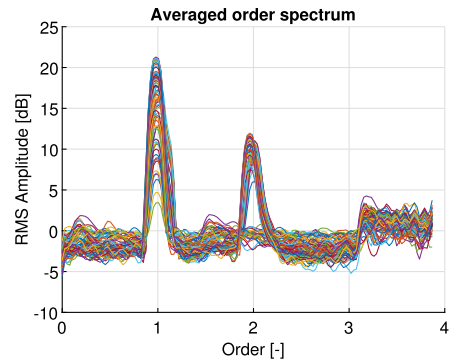
| Designation | Slide bearing damping x_1 | Clutch stiffness x_2 | Friction velocity* x_3 | Clutch damping x_4 |
|--------------|-----------------------------|---------------------------------------|--------------------------|----------------------------|
| Upper limit | 234 N mm s ⁻¹ | 3.45×10^6 N mm ⁻¹ | 10 mm s ⁻¹ | 514.6 N mm s ⁻¹ |
| Medium value | 117.5 N mm s ⁻¹ | 3.16×10^6 N mm ⁻¹ | 5.05 mm s ⁻¹ | 258 N mm s ⁻¹ |
| Lower limit | 1 N mm s ⁻¹ | 2.83×10^6 N mm ⁻¹ | 0.1 mm s ⁻¹ | 1 N mm s ⁻¹ |

* The stiction velocity is also adjusted with 10% of the given friction velocity.

3.2 Design of experiments

The input parameter for the design of experiments (DoE) result from the design space analysis. Three values per design variable are chosen to even identify non-linear correlations, which contains a medium value and rearranged limiting values (see Table 2).

Fig. 9 Averaged order spectrum of the 81 DoE simulation runs related to the THD



Through the preselection of design variables and sampling, the total calculation duration is approximately ≈ 122 h.² The setup is identical to the previous design space analysis, whereas the analysis concentrates on the non-linearity related to the principle of the total harmonic distortion of Sect. 2.3. Figure 9 presents the averaged order spectrum of the 81 runs whose rpm input is scaled so that the first order represents the averaged RMS of the base frequency and the second order the first harmonic. Further integer multiplies are not evaluable here, and the trend of the spectrum is removed to enable a comparison.

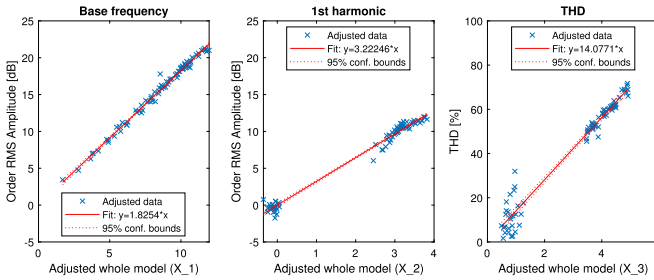
The magnitude of the peaks from the first and second order (compare Sect. 2.3) is used for a multiple regression analysis as well as the total harmonic distortion which is simplified to $THD = 100 \cdot \frac{|P_2|}{|P_1|} [\%]$. Since the simulation resolution is limited by 20 kHz, and the maximum chirp frequency is 5 kHz, an analysis is only possible up to the second order to avoid violating the Nyquist criterion due to the limit of the used sampling frequency. The absolute order magnitudes and the THD given, linear regression analyses are performed, each using a trial function from Equation (18), whereas other trial functions may also be legitimate.

Figure 10 depicts the results of the regression analyses. While the included table (Fig. 10b) presents the detailed regression values, only the most important results are discussed and interpreted in the following sections.

The *F-statistics* with present *p-values* ≈ 0 (not depicted) indicate that the overall regression models are statistically significant as they are < 0.05 . This also proves that the preselection of both design variables and cost functions is suitable, considering the given significance. Since multiple regression factors are present, the *adjusted* correlation coefficient *R-squared* (R_a^2) is used for the analysis. The correlations are for the base frequency $R_a^2 = 0.988$, for the first harmonic $R_a^2 = 0.984$, and for the THD $R_a^2 = 0.959$. Since these values are close to 1, a strong correlation is given for each. In total, this indicates that the regression models are a good fit to the data, further verifying that the trial function and the cost functions are a legitimate selection for the approach. For the base frequency $x_1, x_2, x_3, x_2 : x_3, x_3^2$, and x_4^2 have a significant effect, for the first harmonic $x_3, x_1 : x_3, x_2 : x_4$, and x_3^2 , and for the THD x_3 and x_1^2 . Interpreted and transferred to the design variable names, the slide bearing damping, and the quadratic terms of the stiction and friction velocity most significantly influence the proportion between a dominance of the base frequency related to the – unwanted – presence of the first harmonic.

The clear delineation of the trend (regression) allows for the exclusion of any potential cross-correlations that could lead to model instability. Although the solution changes in re-

²Reference system: CPU 3.6 GHz, 4 cores, 8 logical processors, 32 GB RAM.



(a) Graphical illustration of the regression for the base frequency, the first harmonic, and the THD.

| Variable | Base Frequency | | | | 1 st Harmonic | | | | Total Harmonic Distortion (THD) | | | |
|-----------------|----------------|----------|--------|----------|--------------------------|----------|--------|----------|---------------------------------|----------|--------|----------|
| | Estimate | SE | tStat | pValue | Estimate | SE | tStat | pValue | Estimate | SE | tStat | pValue |
| (Intercept) | 0.0000 | 0.0000 | NaN | NaN | 0.0000 | 0.0000 | NaN | NaN | 0.0000 | 0.0000 | NaN | NaN |
| x1 | 0.0466 | 0.0072 | 6.48 | 1.35e-8 | -0.0004 | 0.0096 | -0.04 | 0.970 | -0.0488 | 0.0705 | -0.69 | 0.492 |
| x2 | 8.83e-6 | 5.09e-7 | 17.33 | 2.92e-26 | 8.93e-7 | 6.79e-7 | 1.31 | 0.193 | 3.84e-6 | 4.99e-6 | 0.77 | 0.445 |
| x3 | 1.8147 | 0.1695 | 10.71 | 4.51e-16 | 3.2174 | 0.2261 | 14.23 | 8.61e-22 | 14.063 | 1.6608 | 8.47 | 3.86e-12 |
| x4 | 0.0060 | 0.0033 | 1.84 | 0.070 | -0.0077 | 0.0044 | -1.76 | 0.082 | -0.0062 | 0.0320 | -0.19 | 0.847 |
| x1:x2 | -1.70e-10 | 2.18e-9 | -0.08 | 0.938 | 1.93e-9 | 2.90e-9 | 0.66 | 0.510 | -5.06e-9 | 2.13e-8 | -0.24 | 0.813 |
| x1:x3 | -0.0005 | 0.0001 | -3.86 | 2.60e-4 | 0.0006 | 0.0002 | 3.13 | 0.003 | -0.0014 | 0.0014 | -1.00 | 0.319 |
| x1:x4 | -2.81e-6 | 2.67e-6 | -1.05 | 0.296 | -3.63e-6 | 3.56e-6 | -1.02 | 0.312 | 2.22e-6 | 2.61e-5 | 0.08 | 0.933 |
| x2:x3 | 3.34e-7 | 5.12e-8 | 6.53 | 1.10e-8 | -1.33e-7 | 6.83e-8 | -1.95 | 0.056 | -7.38e-7 | 5.02e-7 | -1.47 | 0.146 |
| x2:x4 | 3.85e-9 | 9.87e-10 | 3.90 | 2.28e-4 | 3.32e-9 | 1.32e-9 | 2.52 | 0.014 | 6.36e-9 | 9.68e-9 | 0.66 | 0.513 |
| x3:x4 | -0.0007 | 6.28e-5 | -11.82 | 5.93e-18 | 0.0003 | 8.38e-5 | 4.04 | 1.40e-4 | -0.0001 | 0.0006 | -0.17 | 0.866 |
| x1 ² | -0.0001 | 8.32e-6 | -13.45 | 1.40e-20 | -2.07e-5 | 1.11e-5 | -1.86 | 0.067 | 0.0002 | 8.15e-5 | 2.53 | 0.014 |
| x2 ² | -2.33e-12 | 1.57e-13 | -14.80 | 1.20e-22 | -3.78e-13 | 2.10e-13 | -1.80 | 0.076 | -7.19e-14 | 1.54e-12 | -0.05 | 0.963 |
| x3 ² | -0.1914 | 0.0046 | -41.54 | 4.88e-49 | -0.1810 | 0.0061 | -29.45 | 1.10e-39 | -0.6253 | 0.0451 | -13.85 | 3.34e-21 |
| x4 ² | -1.52e-5 | 1.71e-6 | -8.86 | 7.72e-13 | -4.13e-6 | 2.28e-6 | -1.81 | 0.075 | -1.43e-5 | 1.68e-5 | -0.86 | 0.396 |

(b) Results across the signal types presenting the estimates, standard errors (SE), *t*-statistics and *p*-values.

Fig. 10 Application of the multiple regression model using the function *film* of the *Matlab* toolboxes

lation to the absolute values, the characteristic behaviour remains the same. Through the variation of most parameters, including the design space analysis, it is concluded that the simulation runs stably. Potential deviations from the measurement can only stem from the size of the parameter values, or the underlying modelling assumptions, which approximate the present situation insufficiently precisely, e.g. through the simplification of either rigid or flexible bodies. Therefore, it can be excluded that an error fundamentally exists with the applied model assumptions. Solely the accuracy may be reduced. Hence, the fundamental *MBD* model proves to be robust and is accepted as valid. By tuning the appropriate relationship between the slide bearing damping and the stiction and friction velocity, it may also be possible to further optimise the model.

3.3 Validation of the methodology

Applying the design space analysis as a first step, solely utilising the FRF, allows for pre-filtering highly sensitive parameters. In doing so, only linear parameter effects are considered, since one parameter is varied at a time. Regarding high-fidelity and computationally intensive simulations, this approach significantly reduces computational effort. For instance, with 19 parameters, only 38 iterations are required, compared to 3¹⁹ in a full factorial design of experiments with three levels. At the same time, it neglects principal nonlinear cross-correlations between parameters, which may substantially contribute to the system response. Nonetheless, the first step serves as the first indicator during model development, grounded on the assumption of a locally linear system response around a nominal point, related to the parameter dependencies. Thus, small perturbations are expected. This permits the estimation of main effects, which typically dominate the overall system behaviour in early design stages or near an operating point [35]. The use of the FRF for this procedure enables the

physical evaluation of the frequency amplitude information. Building the scalar to a reference curve allows for evaluation in a single scalar value, tailoring it to apply a cost function. The reduction of the effective dimension of the problem through design space analysis enables a more refined nonlinear study of the identified influencing parameters. This aligns with the principle of a progressive model enrichment, using global sensitivities (compare [36]). Therefore, this procedure is considered a valid first step.

As a second step, the design of experiments enables a thorough investigation of the dependencies and cross-correlations among the pre-filtered, sensitive parameters. In the particular case, a three-level full factorial DoE is applied. This approach systematically explores the entire parameter space, ensuring that nonlinear dependencies and interaction effects between parameters are fully captured. Thus, it is assumed to be valid, as it does not neglect any relevant information.

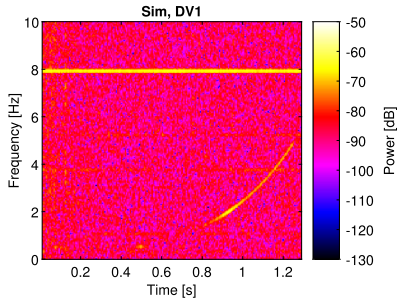
Performing the regression analysis as the third and final step shows that the evaluation based on higher harmonic occurrences and the THD yields a good fit for the regression model. A high statistical significance can be determined with p-values close to zero and adjusted correlation coefficients of $R_a^2 > 0.95$. This finding justifies the application of the principal idea behind the THD as a meaningful basis for the cost function in the DoE and subsequent regression analysis. The analysis of the regression coefficients reveals the presence of nonlinear parameter dependencies, i.e. recognizable as the squared coefficient terms. This supports the utilisation of a multiple linear regression model using a quadratic approximation function in the presented application case.

The principal application of the FRF and THD in this context shall be validated in the following. Figure 11b presents the spectrograms of the frequency-time sequence from the acceleration signal captured in both the simulation and the measurement.

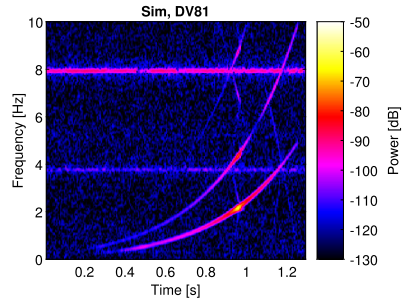
The comparison between simulation results (see Fig. 11a and 11b) and experimental data (see Fig. 11c and 11d) reveals a similar presence of the chirp excitation pattern in both domains, indicating a sound methodological alignment. However, there are some deviations, such as the amplitude level and the occurrence of certain resonances. Notably, the simulation has a persistent resonance near 8 kHz and a weaker one around 4 kHz, which cannot be attributed to a certain feature. Thus, these deviations indicate potential limitations in the current model fidelity, while having only a limited impact on the application of the proposed method. Despite these discrepancies, the characteristic response under increased excitation levels provides valuable insights. In both the simulation and the measurement, higher excitation amplitudes lead to the emergence of harmonic content that reflects system nonlinearities. These nonlinear effects manifest as multiples of the fundamental chirp signal. Suggesting the principle of the THD allows for capturing these effects and making it “measurable”. In contrast, the FRF allows for capturing the classical linear frequency information, such as the natural frequencies. Therefore, the basic application, which uses a logarithmic chirp as the excitation force and subsequently analyses the FRF and THD, is considered valid.

The convergence of the numerical solver is satisfactory, using the Hilber-Hughes-Taylor (HHT) solver algorithm with a tolerance level of 1.0×10^{-7} error size and 5.0×10^{-6} maximum time step size. The principal assumption of rigid or flexible bodies indicates a significant difference in the evaluation of the FRF (see Fig. 12a), while a sample measurement is used to review the present sensitivity of the axial preload (see Fig. 12b), which is identified within the simulation as one highly sensitive parameter.

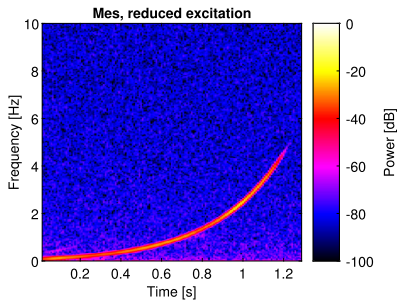
The amplitude levels of Fig. 12a differ for the rigid and flexible approach below 1.5 kHz and at around 2.5 kHz, even though solely rigid body oscillations are present below 5 kHz. As a result, it is concluded that specific effects may already be introduced by the modelling



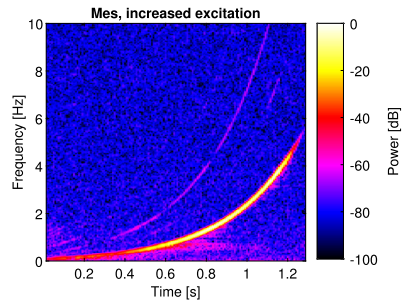
(a) Simulation, DoE of parameter value combination DV_{1} .



(b) Simulation, DoE of parameter value combination DV_{81} .

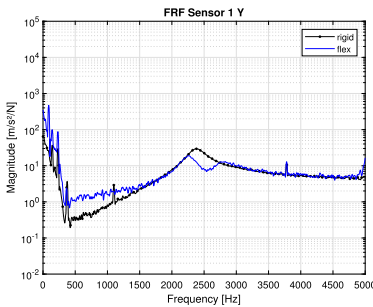


(c) Measurement with low excitation force.

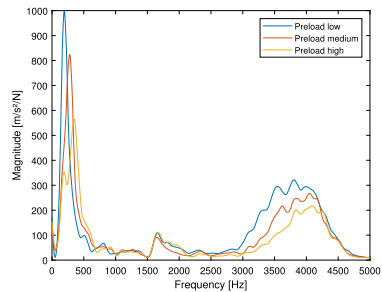


(d) Measurement with high excitation force.

Fig. 11 Frequency-time sequences of the measured and simulated acceleration signal, analysed at the depicted sensor position from Fig. 6c



(a) FRF comparison between rigid and flexible simulation approach.



(b) Measurement with increased axial preload, revealing the sensitivity identified by simulation means.

Fig. 12 Analysis of different scenarios regarding the application of the methodology

assumptions themselves and should, for example, be considered through additional parameters, e.g. the modal damping in this particular case. This indicates that some influences originate purely from the model assumption, and less from the type of analysis. Thus, it

is assumed that the general FRF-based analysis remains applicable even if the modelling assumptions change.

The shift of the resonance frequencies in Fig. 12b under increasing preload is attributed to the accompanying increase of the parameter value, which represents the bearing stiffness. The simulation-based analysis reveals this as a sensitive parameter, while the physical measurement confirms it. Although this is a single sample, it highlights the primary functionality of the approach used.

4 Discussion

First, the design space analysis is used to pre-filter sensitive parameters and verify the model's validity within the given parameter space limits. Since solely one parameter value is changed at a time, it only allows for identifying linear parameter dependencies, while mutual or nonlinear interactions between parameter changes are not captured. However, this serves as an initial indicator for sensitive parameters and reduces the amount of simulations, whereas the subsequent design of experiments ensures that it captures the more complex dependencies. By multiplying the frequency response function of a current parameter state with the reference curve of the nominal state, the design space's cost function yields a scalar value. This value is highly sensitive to even minor changes, as it captures deviations in both frequency and amplitude. Consequently, any alteration in the system response, whether linear or nonlinear, is assumed to be detected through this approach, making it favourable for pre-filtering of sensitive parameters. The application of the frequency response function itself requires identical system conditions over all simulations, which shall be compared. Therefore, the underlying model must have a sufficient degree of maturity and accuracy and requires given parameter values for both the nominal state and the limits. The approach does not apply to fundamentally different or inadequately defined model states.

Second, the design of experiments is applied solely to parameters identified as sensitive in the first step. This enables a full factorial analysis within a reduced parameter space, allowing for the identification of cross-correlations among these parameters while reducing computational effort. It is assumed that these parameters have a decisive influence on the system, which can be justified through simulations and experimental validation. However, the possibility that pre-filtered parameter combinations might influence the system's behaviour is not addressed, leaving this open to future research. The application of the total harmonic distortion along the order domain representation in combination with a logarithmic chirp as excitation signal allows for the identification of the degree of nonlinearity imposed by a certain parameter combination. The total harmonic distortion yields a scalar quantity that can be directly used within the cost function for the design of experiments. In the applied setup, this achieves an adjusted correlation coefficient of $R_a^2 = 0.959$ in the subsequent regression analysis, indicating the functionality of the approach. However, the influence of both structural resonances and higher-order harmonic components beyond the performed analysis requires further testing to exclude potential disturbances.

Third, the applied multiple linear regression is valid for nonlinear systems under the assumption that the relationship between the parameter variables can be assumed to be linear. The quadratic regression model yields the best results for the analysed system. Nevertheless, alternative regression models may also be applicable and could potentially improve an individual analysis.

Currently, the proposed methodology is mainly implemented as a postprocessing step, external to the multi-body dynamic simulation environment, which limits the potential utilisation. For example, integrating and analysing the cost function during a simulation loop

could enhance the applicability of other statistical evaluation possibilities and optimisations. The proposal aims to serve as a basis for future research since no universally applicable validation technique exists. For example, alternative excitation and analysis strategies could be explored within the framework: Using a range of sinusoidal inputs could offer deeper insights into time-domain behaviours such as decay and damping. Similarly, adapting the design of experiments, such as replacing the initial design space analysis with a reduced one or simplifying the subsequent full-factorial design, might yield comparable insights with reduced computational efforts.

5 Conclusion

The proposed methodology enables the efficient identification of sensitive parameters in a nonlinear multi-body dynamic model, whose nonlinearities predominantly arise from contact conditions. The novelty lies in the integration of established methods into a coherent workflow, which comprises three major steps: a design space analysis based on the frequency response function, a design of experiments incorporating total harmonic distortion, and a multiple linear regression analysis. This combination allows for reducing the number of required simulations while capturing the most significant parameters that influence the system behaviour. Therefore, the methodology contributes to a more robust and valid system model, enabling the estimation of virtual and non-accessible parameters by systematically excluding insignificant influences or by evaluating cross-correlations. For example, the application of the methodology reduces the initial number of parameter factors from 19 to four, and the subsequent regression analysis yields an adjusted regression coefficient close to 1 ($R_a^2 = 0.959$), underscoring the significance of the methodology. For validation, comparable setups for both measurement and simulation utilise a small shaker and logarithmic chirp excitation. They reveal matching trends in both the higher harmonic components observable in the response spectrograms and the experimental variation of a parameter identified as sensitive by the methodology. These matching trends support the methodological validity and the fidelity of the underlying model assumptions, since a direct comparison of most parameter sensitivities is infeasible due to their divergent occurrence in measurement and simulation. Primarily, the discrepancies between the simulation results and the experimental results stem from the principal modelling assumption, rather than the parameterisation itself. A key limitation that remains is the underlying assumption of small-amplitude motions and perturbations around equilibrium for the multi-body system. Its application to large-scale dynamics has not been tested and may lose validity in strongly nonlinear systems. Moreover, the robustness against modelling errors and disturbance effects is currently unassessed. Therefore, future research could involve applying the proposed methodology to benchmark systems with either simplified or refined properties and investigating the validity for large motions.

Acknowledgements We gratefully acknowledge Robert Bosch GmbH for providing the resources and supplementary material that enabled this research.

Author contributions Conceptualization, K.S. and D.R.; methodology, K.S., D.L. and I.G.; software, K.S.; validation, K.S.; formal analysis, D.R.; investigation, K.S.; resources, K.S.; data curation, K.S.; writing—original draft preparation, K.S.; writing—review and editing, D.R., I.G. and P.K.; visualization, K.S.; supervision, D.L., I.G., P.K. and D.R.; project administration, K.S., D.L. and D.R. All authors have read and agreed to the published version of the manuscript.

Funding information Open Access funding enabled and organized by Projekt DEAL. The author(s) received no financial support for the research, authorship, and/or publication of this article.

Data availability The data supporting this study are not publicly available, but access may be granted upon reasonable request and with approval from Robert Bosch GmbH.

Declarations

Competing interests The authors Kevin Steinbach and Dominik Lechler were employed by the company Robert Bosch GmbH. The remaining authors declare that the research was conducted in the absence of any commercial or financial relationships that could be construed as a potential conflict of interest. Apart of that, the authors declared no potential conflicts of interest with respect to the research, authorship, and/or publication of this article.

Open Access This article is licensed under a Creative Commons Attribution 4.0 International License, which permits use, sharing, adaptation, distribution and reproduction in any medium or format, as long as you give appropriate credit to the original author(s) and the source, provide a link to the Creative Commons licence, and indicate if changes were made. The images or other third party material in this article are included in the article's Creative Commons licence, unless indicated otherwise in a credit line to the material. If material is not included in the article's Creative Commons licence and your intended use is not permitted by statutory regulation or exceeds the permitted use, you will need to obtain permission directly from the copyright holder. To view a copy of this licence, visit <http://creativecommons.org/licenses/by/4.0/>.

References

- Pigorini, F., Gugliotta, A., Sinokrot, T., Shabana, A.A.: Experimental validation of non-linear multi-body railroad vehicle system algorithms. *Proc. Inst. Mech. Eng. Part K, J. Multi-Body Dyn.* **221**(4), 505–513 (2007). <https://doi.org/10.1243/14644193jmbd107>
- Parra, A., Cagigas, D., Zubizarreta, A., Rodriguez, A.J., Prieto, P.: Modelling and validation of full vehicle model based on a novel multibody formulation. In: *IECON 2019 - 45th Annual Conference of the IEEE Industrial Electronics Society*, vol. 1, pp. 675–680. IEEE, Lisbon (2019). <https://doi.org/10.1109/iecon.2019.8926854>
- Kloppogge, P., Sluijs, J.P., Petersen, A.C.: A method for the analysis of assumptions in model-based environmental assessments. *Environ. Model. Softw.* **26**(3), 289–301 (2011). <https://doi.org/10.1016/j.envsoft.2009.06.009>
- Smith, E., Szidarovsky, F., Karnavas, W., Bahill, A.T.: Sensitivity analysis, a powerful system validation technique. *Open Cybern. Syst. J.* **2**, 39–56 (2007). <https://doi.org/10.2174/1874110X00802010039>
- Dimov, I., Georgieva, R.: *Multidimensional Sensitivity Analysis of Large-Scale Mathematical Models*, pp. 137–156. Springer, New York (2013). https://doi.org/10.1007/978-1-4614-7172-1_8
- Gatti, G., Brennan, M.J., Kovacic, I.: On the interaction of the responses at the resonance frequencies of a nonlinear two degrees-of-freedom system. *Phys. D: Nonlinear Phenom.* **239**(10), 591–599 (2010). <https://doi.org/10.1016/j.physd.2010.01.006>
- Carri, A., Ewins, D.J.: Assessment and validation of nonlinear identification techniques using simulated numerical and real measured data. In: Allemang, R. (ed.) *Topics in Modal Analysis II*, vol. 8, pp. 285–298. Springer, Cham (2014). <https://doi.org/10.1007/978-3-319-04774-4>
- Luo, A.C.J.: *Bifurcation and Stability in Nonlinear Dynamical Systems*. Springer, Cham (2019). <https://doi.org/10.1007/978-3-030-22910-8>
- Arnold, D.N.: *Stability, Consistency, and Convergence of Numerical Discretizations*, pp. 1358–1364. Springer, Berlin (2015). https://doi.org/10.1007/978-3-540-70529-1_407
- Bauchau, O.A.: Computational schemes for flexible, nonlinear multi-body systems. *Multibody Syst. Dyn.* **2**(2), 169–225 (1998). <https://doi.org/10.1023/a:1009710818135>
- Renardy, M., Wessler, T., Blemker, S., Linderman, J., Peirce, S., Kirschner, D.: Data-driven model validation across dimensions. *Bull. Math. Biol.* **81**(6), 1853–1866 (2019). <https://doi.org/10.1007/s11538-019-00590-4>
- Mokhtari, F., Imanpour, A.: Hybrid data-driven and physics-based simulation technique for seismic analysis of steel structural systems. *Comput. Struct.* **295**, 107286 (2024). <https://doi.org/10.1016/j.compstruc.2024.107286>
- Zhang, X.P., Ahmed, H., Yao, Z.: Multi-body contact modeling and statistical experimental validation for hub-bearing unit. *Tribol. Int.* **36**(7), 505–510 (2003). [https://doi.org/10.1016/s0301-679x\(02\)00186-x](https://doi.org/10.1016/s0301-679x(02)00186-x)
- Kerschen, G., Worden, K., Vakakis, A.F., Golinval, J.-C.: Past, present and future of nonlinear system identification in structural dynamics. *Mech. Syst. Signal Process.* **20**(3), 505–592 (2006). <https://doi.org/10.1016/j.ymsp.2005.04.008>

15. Hunt, K.H., Crossley, F.R.E.: Coefficient of restitution interpreted as damping in vibroimpact. *J. Appl. Mech.* **42**(2), 440–445 (1975). <https://doi.org/10.1115/1.3423596>
16. Rill, G., Schaeffer, T., Borchsenius, F.: *Grundlagen und Computergerechte Methodik der Mehrkörper-simulation: Vertieft in Matlab-Beispielen, Übungen und Anwendungen.* Springer, Wiesbaden (2023). <https://doi.org/10.1007/978-3-658-41968-4>
17. Pennestrì, E., Rossi, V., Salvini, P., Valentini, P.P.: Review and comparison of dry friction force models. *Nonlinear Dyn.* **83**(4), 1785–1801 (2015). <https://doi.org/10.1007/s11071-015-2485-3>
18. Johansson, K., Canudas-de-Wit, C.: Revisiting the lugre friction model. *IEEE Control Syst.* **28**(6), 101–114 (2008). <https://doi.org/10.1109/mcs.2008.929425>
19. Olsson, H., Åström, K.J., Wit, C., Gäfvert, M., Lischinsky, P.: Friction models and friction compensation. *Eur. J. Control* **4**(3), 176–195 (1998). [https://doi.org/10.1016/s0947-3580\(98\)70113-x](https://doi.org/10.1016/s0947-3580(98)70113-x)
20. Hertz, H.: Über die Berührung fester elastischer Körper. *J. Reine Angew. Math.* **92**, 156–171 (1882)
21. Kunert, K.: Spannungsverteilung im halbraum bei elliptischer flächenpressungsverteilung über einer rechteckigen druckfläche. *Forsch Ing-Wes* **27**, 165–174 (1961). <https://doi.org/10.1007/BF02561354>
22. Wang, Q.J., Chung, Y.-W. (eds.): *Hertzian Contact of Cylindrical Surfaces*, pp. 1662–1662. Springer, Boston (2013). https://doi.org/10.1007/978-0-387-92897-5_100658
23. Flores, P.: Comparison of different contact force models for low and moderate impact velocities: Numerical and experimental analysis in: *New Trends in Mechanism and Machine Science. Mechanisms and Machine Science* pp. 549–556 Springer, Dordrecht
24. Software, M.S.C.: *MSC Adams User’s Guide.* MSC Software Corporation (2023). <https://www.mscsoftware.com/product/adams> Accessed 2024-11-25
25. The MathWorks, I.: *Matlab 2022 Documentation.* (2022). Accessed: 2024-11-25. <https://www.mathworks.com/help/matlab/>
26. Allemang, R., Avitabile, P. (eds.): *Handbook of Experimental Structural Dynamics.* Springer, New York (2022). <https://doi.org/10.1007/978-1-4614-4547-0>.
27. Comparin, R.J., Singh, R.: Non-linear frequency response characteristics of an impact pair. *J. Sound Vib.* **134**(2), 259–290 (1989). [https://doi.org/10.1016/0022-460x\(89\)90652-4](https://doi.org/10.1016/0022-460x(89)90652-4)
28. Jazar, R.N., Marzbani, H.: *Frequency Response* pp. 211–272. Springer, Cham (2023). https://doi.org/10.1007/978-3-031-43486-0_7
29. Westermo, B., Udvardia, F.: Periodic response of a sliding oscillator system to harmonic excitation. *Earthq. Eng. Struct. Dyn.* **11**(1), 135–146 (1983). <https://doi.org/10.1002/eqe.4290110111>
30. Meirovitch, L.: *Fundamentals of Vibrations*, 1st edn. Waveland Press, Incorporated, Long Grove (2010)
31. Vakakis, A.F., Manevitch, L.I., Mikhlin, Y.V., Pilipchuk, V.N., Zevin, A.A.: *Normal Modes and Localization in Nonlinear Systems.* Wiley Series in Nonlinear Science. Wiley-VCH Verlag, Weinheim (2008)
32. Shmilovitz, D.: On the definition of total harmonic distortion and its effect on measurement interpretation. *IEEE Transactions on Power Delivery* **20**(1), 526–528 (2005). <https://doi.org/10.1109/TPWRD.2004.839744>
33. Brandt, A.: *Noise and Vibration Analysis: Signal Analysis and Experimental Procedures.* Wiley, Hoboken (2011). <https://doi.org/10.1002/9780470978160>
34. Steinbach, K., Lechler, D., Kraemer, P., Groß, I., Reith, D.: A novel approach to predict the structural dynamics of e-bike drive units by innovative integration of elastic multi-body-dynamics. *Vehicles* **5**(4), 1227–1253 (2023)
35. Saltelli, A., Ratto, M., Andres, T., Campolongo, F., Cariboni, J., Gatelli, D., Saisana, M., Tarantola, S.: *Global Sensitivity Analysis. The Primer.* Wiley, Hoboken (2007). <https://doi.org/10.1002/9780470725184>
36. Pianosi, F., Beven, K., Freer, J., Hall, J.W., Rougier, J., Stephenson, D.B., Wagener, T.: Sensitivity analysis of environmental models: a systematic review with practical workflow. *Environ. Model. Softw.* **79**, 214–232 (2016). <https://doi.org/10.1016/j.envsoft.2016.02.008>